Supporting Information

Azobenzene-functionalized graphene nanoribbons: bottom-up synthesis, photoisomerization behaviour and self-assembled structures

Zhichun Shangguan, Chunyang Yu, Chen Li, Xianhui Huang, Yiyong Mai* and Tao Li *

School of Chemistry and Chemical Engineering, Frontiers Science Center for Transformative Molecules, Key Laboratory of Thin Film and Microfabrication (Ministry of Education), Key Laboratory of Electrical Insulation and Thermal Ageing, Shanghai Jiao Tong University, 800 Dongchuan Road, Shanghai 200240, P. R. China.
E-mail: Yiyong Mai mai@sjtu.edu.cn, Tao Li litao1983@sjtu.edu.cn

1. Experiments

1.1 Synthetic procedures of monomer 1 and monomer 2

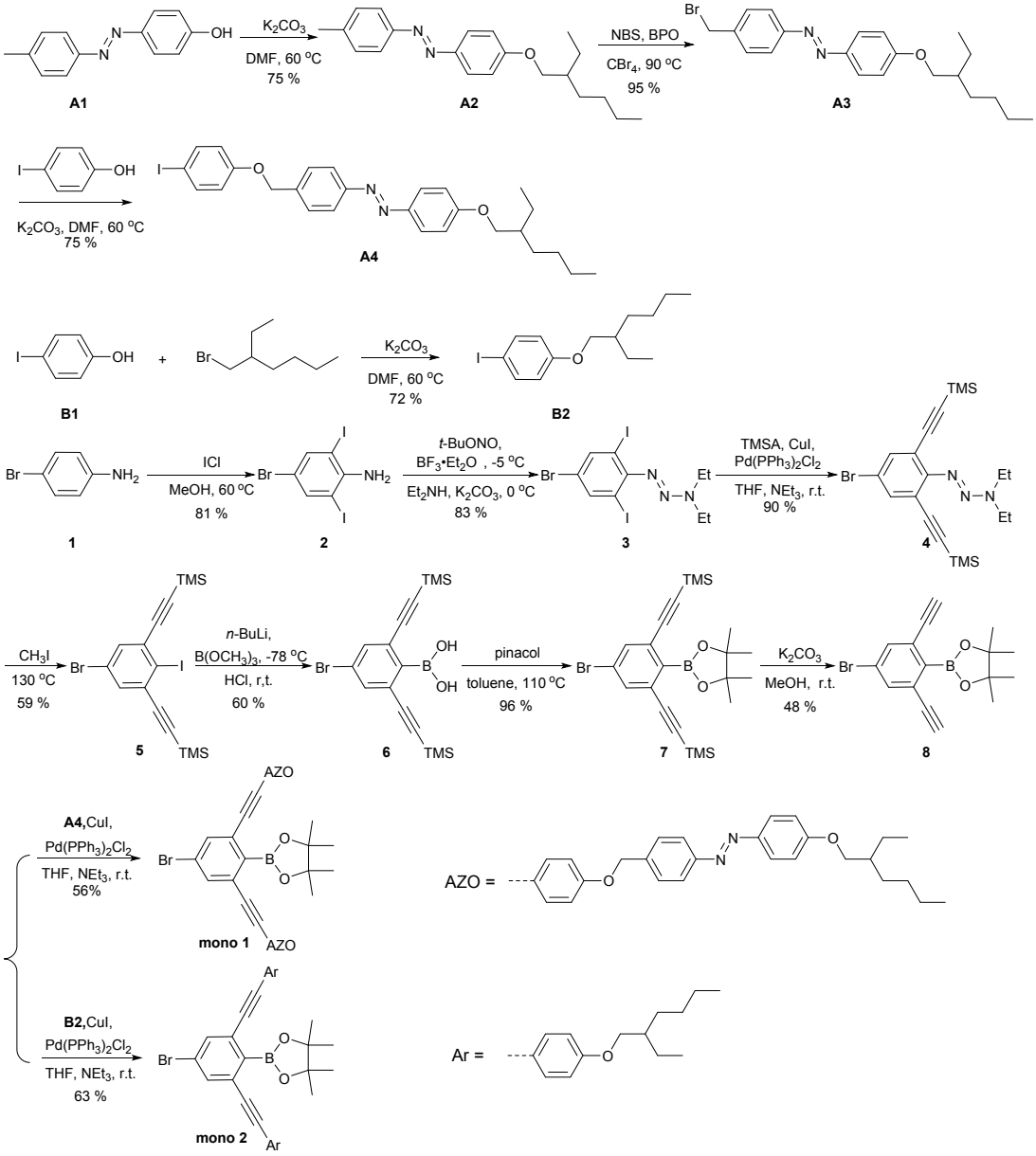

Scheme S1 Synthesis of monomer 1 and monomer 2.

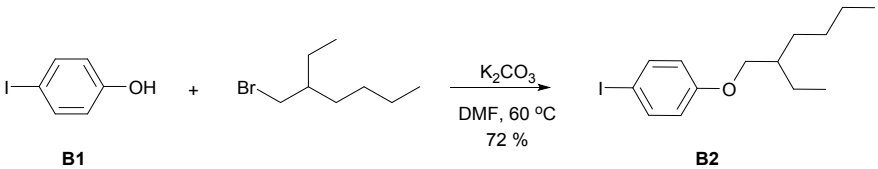

A mixture of compound B1 (5.0 g, 22.7 mmol, 1.0 equiv.) and K_2CO_3 (6.3 g, 45.4 mmol, 2.0 equiv.) in DMF (50 mL) was stirred overnight at 60 ℃ under a nitrogen atmosphere. The reaction mixture was extracted with DCM, dried over Na_2SO_4, filtered, and concentrated by evaporation. The crude residue was purified by silica gel chromatography (hexane/DCM 5:1) to give pure product B2 as a colorless oil (5.4 g, 72 % yield).

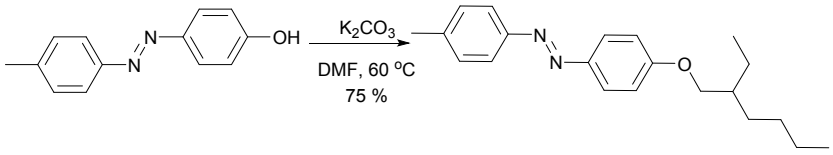

A1 A2

A mixture of compound A1 (5.0 g, 23.6 mmol, 1.0 equiv.) and K_2CO_3 (6.5 g, 47.2 mmol, 2.0 equiv.) in DMF (50 mL) was stirred overnight at 60 ℃ under a nitrogen atmosphere. The reaction mixture was extracted with DCM, dried over Na_2SO_4, filtered, and concentrated by evaporation. The crude residue was purified by silica gel chromatography (hexane/DCM 5:1) to give pure product A2 as an orange oil (5.7 g, 75 % yield).

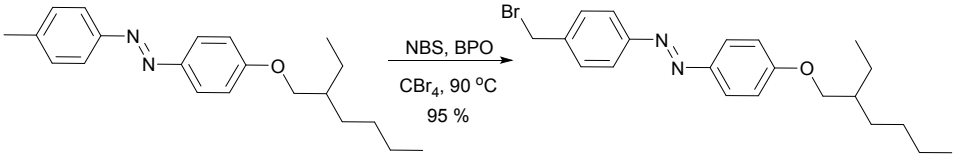

A2 A3

A mixture of compound A2 (5.0 g, 15.4 mmol, 1.0 equiv.) and N-Bromosuccinimide (2.7 g, 15.4 mmol, 1.0 equiv.) was dissolved in CBr_4 (50 mL) under a nitrogen atmosphere, and then a small amount of BPO was added to the mixture in one portion. The reaction was heated to reflux overnight. The reaction mixture was filtered, washed with CBr_4 and concentrated by evaporation to give crude product A3 as an orange oil (5.9 g, 95 % yield). The crude product was directly used for the next step without purification.

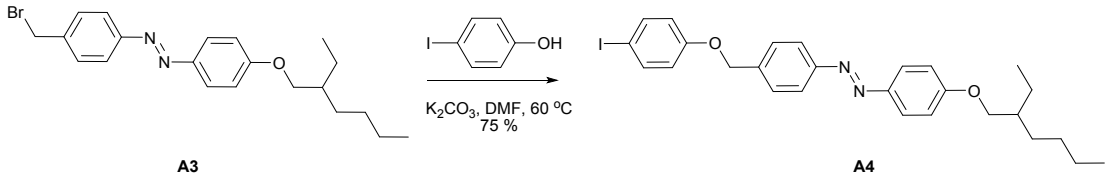

A3 A4

A mixture of crude compound A3 (5.9 g, 14.6 mmol, 1.0 equiv.) and K_2CO_3 (4.0 g, 29.3 mmol, 2.0 equiv.) in DMF (50 mL) was stirred overnight at 60 ℃ under a nitrogen atmosphere. The reaction mixture was extracted with DCM, dried over Na_2SO_4, filtered, and concentrated by evaporation. The crude residue was purified by silica gel chromatography (hexane/DCM 5:1) to give pure product A4 as an orange solid (5.9 g, 75 % yield). ^{1}H NMR (400 MHz, $CDCl_3$) δ 7.89 (dd, *J* = 12.3, 8.6 Hz, 4H), 7.55 (d, *J* = 8.8 Hz, 2H), 7.51 (d, *J* = 8.3 Hz, 2H), 7.00 (d, *J* = 8.9 Hz, 2H), 6.75 (d, *J* = 8.9 Hz, 2H), 5.08 (s, 2H), 3.92 (d, *J* = 7.2 Hz, 2H), 1.76 (m, 1H), 1.56 – 1.38 (m, 4H), 1.33 (m, 4H), 0.93 (m, 6H).

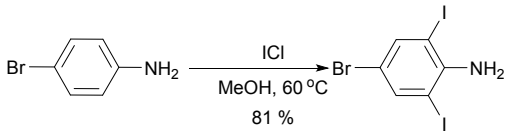

1 2

4-bromoaniline (10 g, 0.058 mol, 1.0 equiv.) and iodine monochloride (25 g, 0.15 mol, 2.65 equiv.) are reacted in 100 mL of MeOH. The mixture was stirred overnight at 60 ℃, then quenched with saturated $Na_2S_2O_3$ solution and then extracted with EtOAc. The organic phase was washed with brine, dried over Na_2SO_4, filtered, and concentrated by evaporation. The crude residue was purified by silica gel chromatography (hexane/DCM 5:1) to give pure product 2 as a white solid (20

g, 81 % yield). ^{1}H NMR (400 MHz, $CDCl_3$) δ 7.73 (s, 2H), 4.63 (s, 2H), corresponding to previous reports[1].

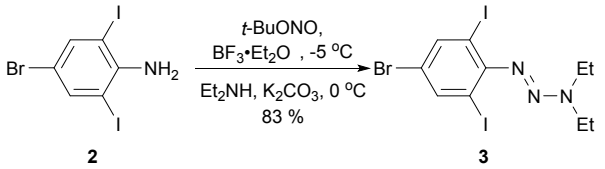

Compound 2 (20 g, 0.047 mol, 1.0 equiv.) was dissolved in 200 mL anhydrous THF and then the solution was cooled to -40 ℃. $BF_3 \cdot Et_2O$ (10 g, 0.070 mol, 1.5 equiv.) was added to the solution. Subsequently, *t*-BuONO (6.3 g, 0.061 mol, 1.3 equiv.) was added dropwise and the mixture was stirred at -5 ℃ for 1 h. Cold Et_2O was added to the mixture that was then filtered and washed with cold Et_2O to give a yellow solid. The yellow solid was added in one portion to a solution of diethylamine (8.6 g, 0.12 mol, 2.5 equiv.) and K_2CO_3 (32 g, 0.24 mol, 5.0 equiv.) in 1:2 CH_3CN/water (300 mL). The reaction mixture was stirred at 0 °C for 30 min and then extracted with DCM. The organic phase was washed with brine, dried over Na_2SO_4, filtered, and concentrated by evaporation. The crude residue was purified by silica gel chromatography (hexane/DCM 5:1) to give pure product 3 as a brown oil (19.8 g, 83 % yield). ^{1}H NMR (400 MHz, $CDCl_3$) δ 7.97 (s, 2H), 3.76 (q, 4H), 1.36 – 1.29 (m, 6H), corresponding to previous reports[2].

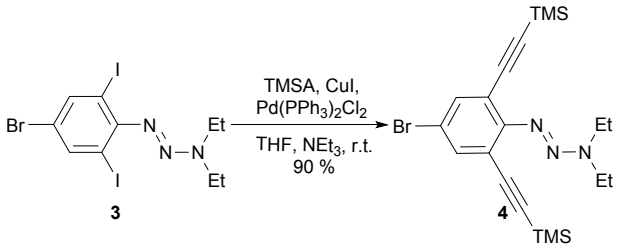

A mixture of compound 3 (19.8 g, 0.039 mol, 1.0 equiv.), trimethylsilylacetylene (11.5 g, 0.12 mol, 3.0 equiv.), $Pd(PPh_3)_2Cl_2$ (680 mg, 0.97 mmol, 0.025 equiv.) and CuI (370 mg, 1.95 mmol, 0.05 equiv.) in THF (200 mL) and triethylamine (50 mL) was stirred at room temperature overnight under a nitrogen atmosphere. The reaction mixture was filtered, and the filtrate was concentrated under reduced pressure. The crude residue was purified by silica gel chromatography (hexane/DCM 5:1) to give pure product 4 as a brown oil (15.7 g, 90 % yield). ^{1}H NMR (400 MHz, $CDCl_3$) δ 7.52 (s, 2H), 0.19 (s, 18H). ^{13}C NMR (101 MHz, $CDCl_3$) δ 153.99, 136.18, 118.10, 115.86, 101.82, 98.56, -0.15.

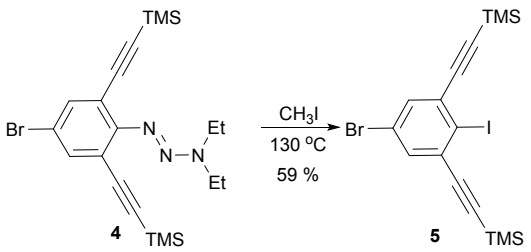

Compound 4 (15.7 g, 0.035 mol, 1.0 equiv.) was dissolved in iodomethane (100 g, 0.70 mol, 20 equiv.) and the solution was heated in a sealed tube at 130 °C for 24 h. The reaction mixture was concentrated under reduced pressure and the residue was purified by silica gel chromatography (hexane/DCM 10:1) to give pure product 5 as a white semisolid (9.8 g, 59 % yield). ^{1}H NMR (400

MHz, $CDCl_3$) δ 7.49 (s, 2H), 0.28 (s, 18H). ^{13}C NMR (101 MHz, $CDCl_3$) δ 134.58, 132.38, 121.06, 106.07, 105.30, 100.72, -0.36.

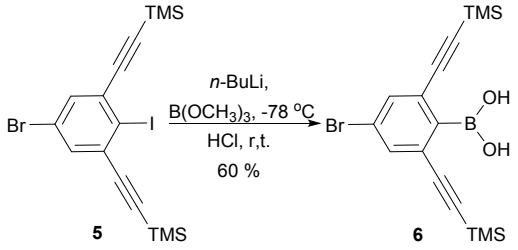

Compound 5 (9.8 g, 20.6 mmol, 1.0 equiv.) was dissolved in 100 mL anhydrous THF and then the solution was cooled to -78 ℃ under a nitrogen atmosphere. *n*-BuLi (8.2 mL, 20.6 mmol, 2.50 M, 1.0 equiv.) was added dropwise to the solution. After stirred for 30 min at –78 °C, trimethyl borate (2.1 g, 20.6 mmol, 1 equiv.) was added and then the mixture was removed from the cooling bath. After stirred for 30 min at room temperature, the reaction mixture was quenched with 2 N HCl and extracted with DCM. The organic phase was washed with brine, dried over Na_2SO_4, filtered, and concentrated by evaporation. The crude residue was purified by silica gel chromatography (hexane/DCM 3:1) to give pure product 6 as a white semisolid (4.86 g, 60 % yield). ^1H NMR (400 MHz, $CDCl_3$) δ 7.66 (s, 2H), 6.98 (s, 2H), 0.29 (s, 18H). ^{13}C NMR (101 MHz, $CDCl_3$) δ 136.46, 129.21, 123.93, 103.93, 101.92, -0.53.

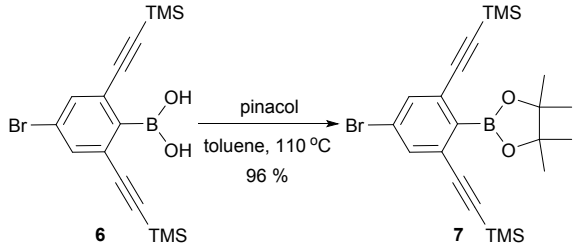

A mixture of compound 6 (4.86 g, 12.4 mmol, 1.0 equiv.) and pinacol (1.46 g, 12.4 mmol, 1.0 equiv.) in toluene (50 mL) was stirred for 2 h at reflux under a nitrogen atmosphere. The reaction mixture was concentrated under reduced pressure and the residue was purified by silica gel chromatography (hexane/DCM 5:1) to give pure product 7 as a white semisolid (5.65 g, 96 % yield). ^1H NMR (400 MHz, $CDCl_3$) δ 7.54 (s, 2H), 1.41 (s, 12H), 0.22 (s, 18H).

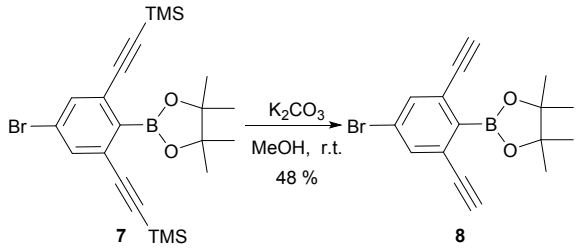

A mixture of compound 7 (5.65 g, 11.9 mmol, 1.0 equiv.) and K_2CO_3 (4.92 g, 35.7 mmol, 3.0 equiv.) in MeOH (50 mL) was stirred for 2 h at room temperature under a nitrogen atmosphere. The reaction mixture was extracted with DCM, dried over Na_2SO_4, filtered, and concentrated by evaporation. The crude residue was purified by silica gel chromatography (hexane/DCM 5:1) to give pure product 8 as a white semisolid (1.89 g, 48 % yield). ^1H NMR (400 MHz, $CDCl_3$) δ 7.60 (s, 2H), 3.15 (s, 2H), 1.40 (s, 12H).

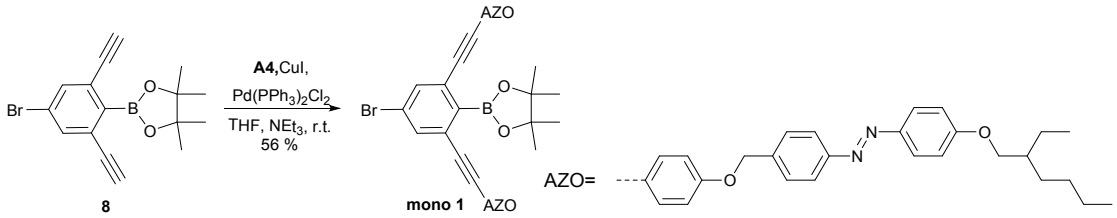

A mixture of compound 8 (331 mg, 1 mmol, 1.0 equiv.), compound A4 (1.19 g, 2.2 mmol, 2.2 equiv.), $Pd(PPh_3)_2Cl_2$ (17.5 mg, 0.025 mmol, 0.025 equiv.) and CuI (9.5 mg, 0.05 mmol, 0.05 equiv.) in THF (20 mL) and triethylamine (10 mL) was stirred at room temperature overnight under a nitrogen atmosphere. The reaction mixture was filtered, and the filtrate was concentrated under reduced pressure. The crude residue was purified by silica gel chromatography (hexane/EA 20:1) to give pure product 9 as an orange solid (650 mg, 56 % yield). ^{1}H NMR (400 MHz, $CDCl_3$) δ 7.90 (t, *J* = 8.2 Hz, 8H), 7.59 (s, 2H), 7.53 (d, *J* = 8.4 Hz, 4H), 7.44 (d, *J* = 8.3 Hz, 4H), 7.00 (d, *J* = 9.0 Hz, 4H), 6.95 (d, *J* = 8.8 Hz, 4H), 5.11 (s, 4H), 3.91 (d, *J* = 6.0 Hz, 4H), 1.83 – 1.69 (m, 2H), 1.58 – 1.39 (m, 8H), 1.37 (s, 12H), 1.35 – 1.27 (m, 8H) 0.92 (m, 12H). ^{13}C NMR (101 MHz, $CDCl_3$) δ 162.13, 158.94, 152.57, 146.81, 138.69, 133.84, 133.16, 128.73, 127.99, 124.85, 122.85, 115.44, 115.00, 114.79, 91.77, 87.12, 84.54, 70.89, 69.65, 39.37, 30.53, 29.12, 25.06, 23.88, 23.09, 14.16, 11.18.

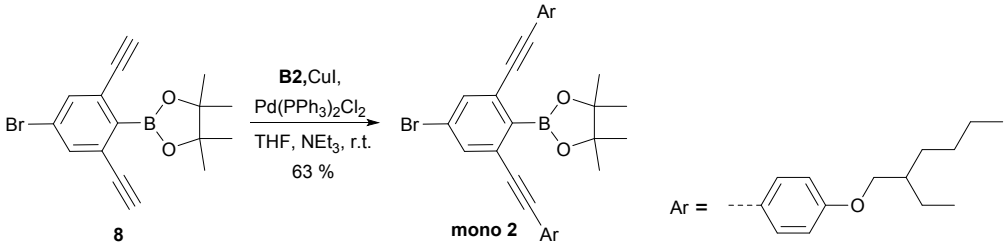

A mixture of compound 8 (331 mg, 1 mmol, 1.0 equiv.), compound B2 (728 mg, 2.2 mmol, 2.2 equiv.), $Pd(PPh_3)_2Cl_2$ (17.5 mg, 0.025 mmol, 0.025 equiv.) and CuI (9.5 mg, 0.05 mmol, 0.05 equiv.) in THF (20 mL) and triethylamine (10 mL) was stirred at room temperature overnight under a nitrogen atmosphere. The reaction mixture was filtered, and the filtrate was concentrated under reduced pressure. The crude residue was purified by silica gel chromatography (hexane/DCM 4:1) to give pure product 10 as a yellow oil (465 mg, 63 % yield). ^{1}H NMR (400 MHz, $CDCl_3$) δ 7.56 (s, 2H), 7.43 (d, J = 8.9 Hz, 4H), 6.85 (d, J = 8.9 Hz, 4H), 3.81 (d, J = 5.8 Hz, 4H), 1.73 – 1.67 (m, 2H), 1.45 (m, 8H), 1.36 (s, 12H), 1.31 (m, 8H), 0.91 (m, 12H), corresponding to previous reports[2].

2. Characterizations of chemical structures of GNR-AZOs

2.1 GPC Data

PDAPP-AZOs	M_n (g/mol)	M_w (g/mol)	PDI	GNR length (nm)
PDAPP-AZO1	6,428	8,622	1.34	2.9
PDAPP-AZO2	4754	7012	1.47	3.3

Table S1 GPC Data of PDAPP-AZOs Samples and Lengths of the Corresponding GNR-AZOs.

2.2 FTIR spectroscopy

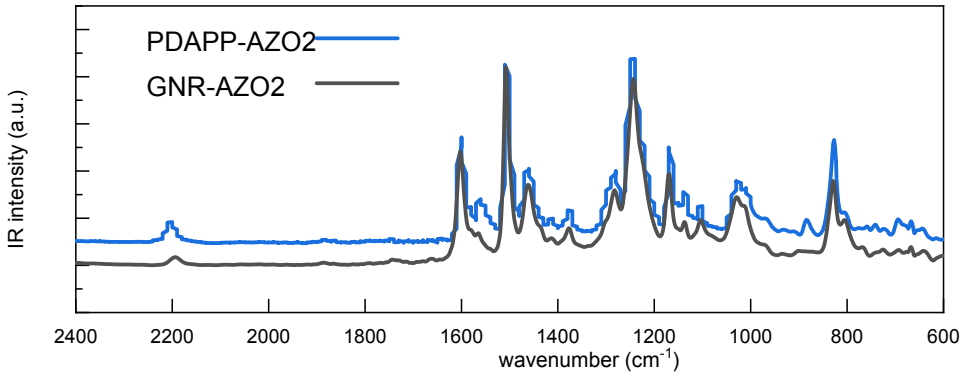

Fig. S1 IR spectra of PDAPP-AZO2 (blue) and GNR-AZO2 (black).

2.3 Raman spectroscopy

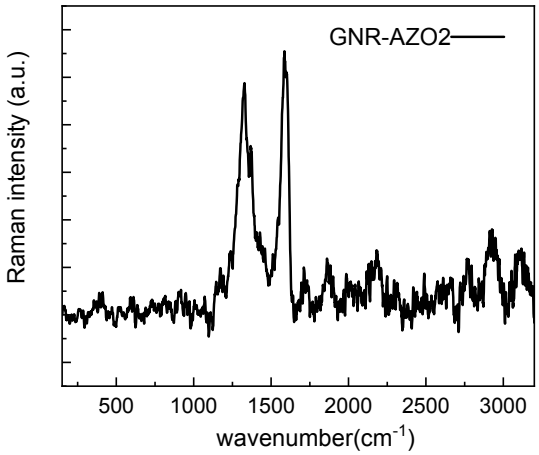

Fig. S2 Raman spectrum of GNR-AZO2.

2.4 Calculate the grafting rates of GNR-AZOs

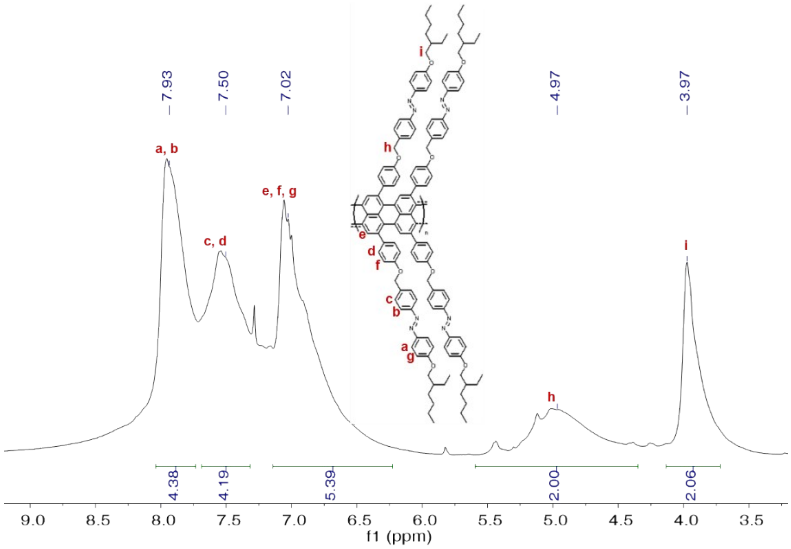

Fig. S3 ^{1}H NMR spectra of GNR-AZO1 in $CDCl_3$.

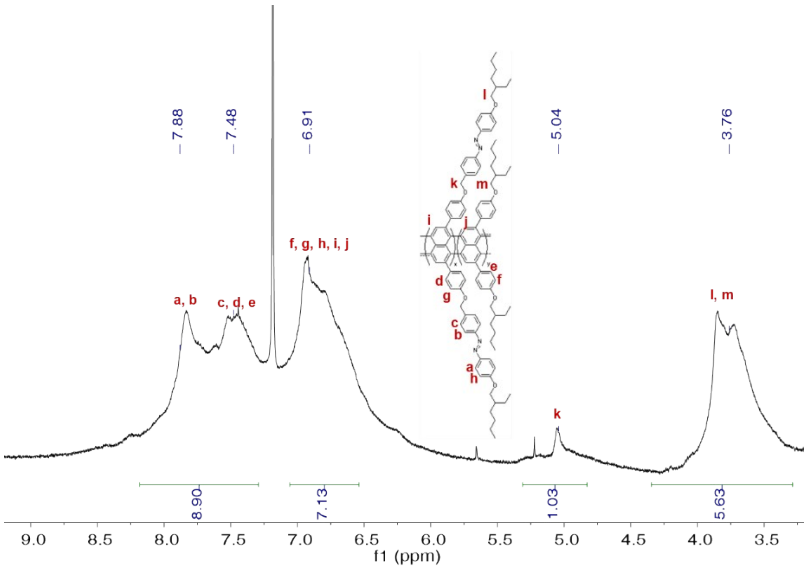

Fig. S4 ^{1}H NMR spectra of GNR-AZO2 in $CDCl_3$.

The grafting rates of GNR-AZO1 and GNR-AZO2 can be calculated by the integral ratio between 4.97 ppm and 3.97 ppm. For GNR-AZO1, the ratio between 4.97 ppm and 3.97 ppm was 1: 1, which means all side chains of GNR were grafted with azobenzene group. For GNR-AZO2, the ratio was 1: 5.63, which means only 17.8 % side chains of GNR were grafted with azobenzene group.

2.5 Photoluminescence spectra

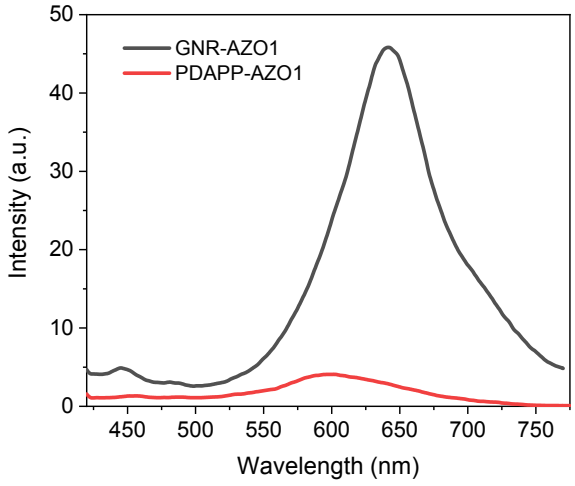

Fig. S5 Photoluminescence spectra of PDAPP-AZO1 and GNR-AZO1 in THF.

3. Photoisomerization of GNR-AZOs

3.1 Calculate the *trans*-isomer ratio in PSS state

The conversion ratios for the *trans/cis* forms of azobenzene under light irradiations were estimated according to literatures.[3] In order to clearly show the change in the absorption spectrum due to the photoisomerization of the azobenzene group in GNR-AZOs, the absorbance due to the

GNRs backbone[2] was subtracted from the data. The *trans*-isomer ratio in PSS state can be roughly estimated by the following formula:

$$\alpha_{trans}\% = (A_t - A_{GNRs})/(A_0 - A_{GNRs})$$

A_{GNRs}: Absorbance of GNRs backbone at 350 nm, A_t: Absorbance of GNR-AZOs at 350 nm at time t, A_0: Absorbance of GNR-AZOs at 350 nm at time 0 (initial).

For GNR-AZO1, the *trans*-isomer ratio in PSS state was estimated to 15 % and thus 85 % of the *trans*-isomer was transformed into the *cis*-isomer after UV light irradiation in solution state. Similarly, 37 % of the *trans*-isomer was transformed into the *cis*-isomer after UV light irradiation in film state.

3.2 UV-vis absorption spectrum

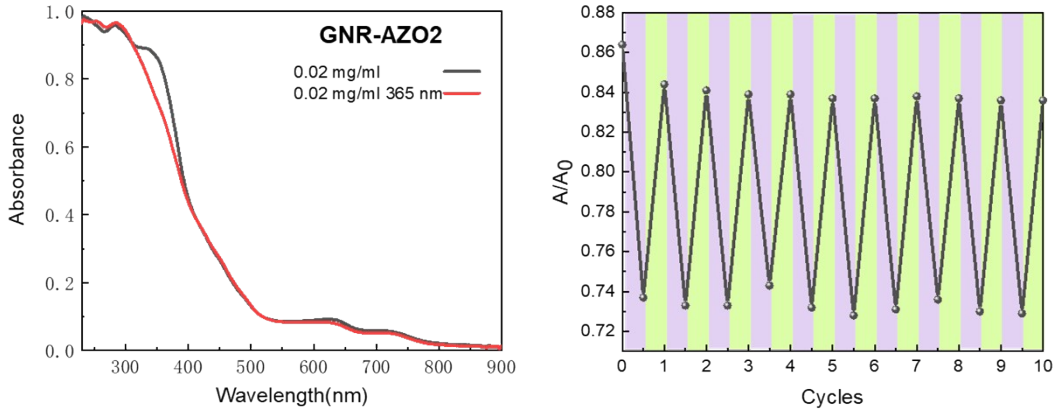

Fig. S6 (left) UV-vis absorption changes of GNR-AZO2 solution (0.02 mg/ml in THF) during the irradiation with UV light (365 nm). (right) The reversible variations of the absorption intensity at 350 nm for GNR-AZO2 solution after alternating UV (365 nm for 20 s) and visible light (500 nm for 40 s) irradiations.

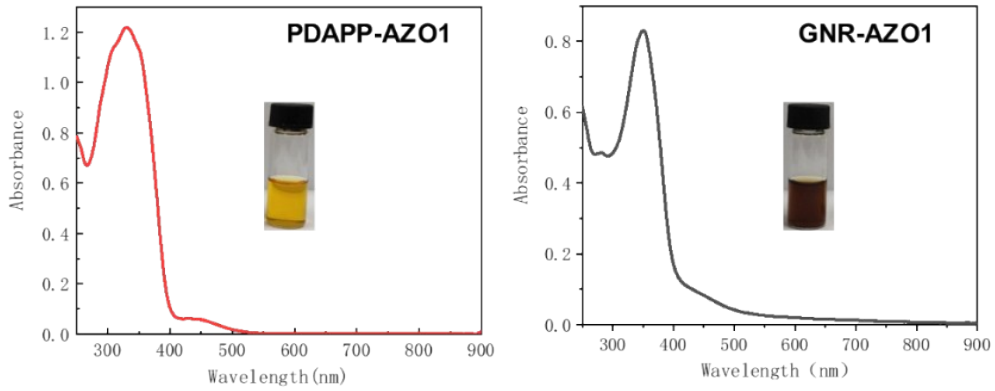

Fig. S7 (left) UV-vis absorption spectrum of PDAPP-AZO1 solution (0.02 mg/ml in THF) and (right) UV-vis absorption spectrum of GNR-AZO1 solution (0.02 mg/ml in THF). The inserted pictures are optical photos of PDAPP-AZO1 (1 mg/ml in THF) and GNR-AZO1 (1 mg/ml in THF), respectively.

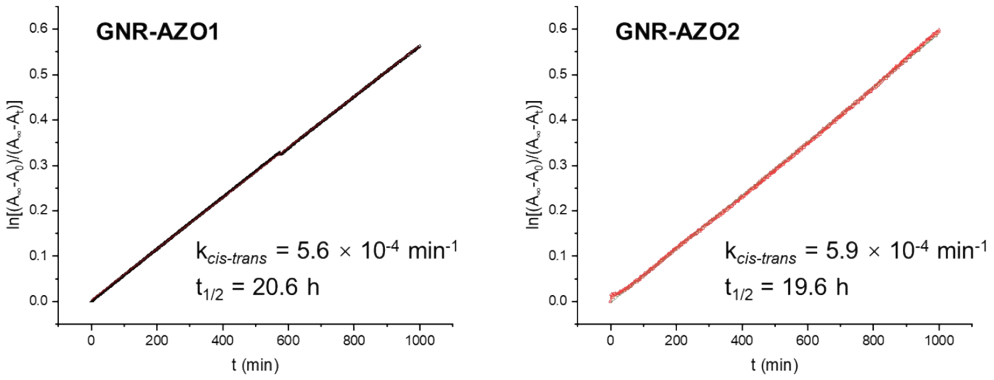

Fig. S8 First-order *cis-trans* isomerization kinetic of (left) GNR-AZO1 and (right) GNR-AZO2 in THF solution at 25 ℃.

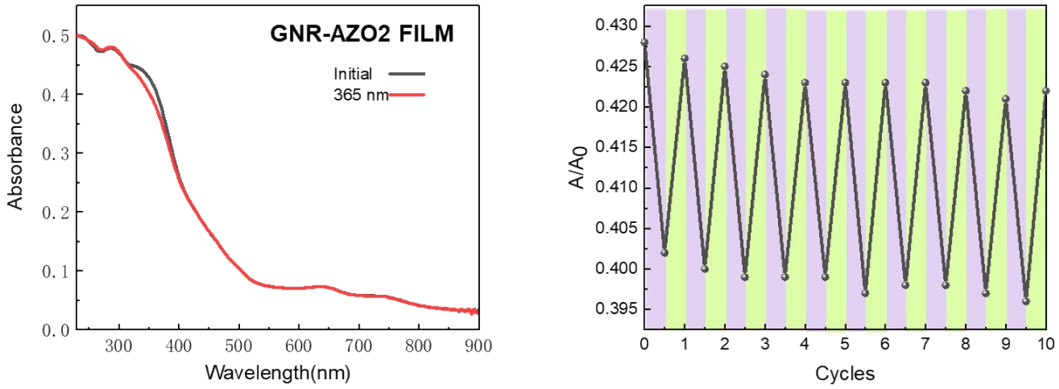

Fig. S9 (left) UV-vis absorption changes of GNR-AZO2 film (by spin-coating in 40 mg/mL chlorobenzene) during the irradiation with UV light (365 nm) (right) The reversible variations of the absorption intensity at 350 nm for GNR-AZO2 film after alternating UV (365 nm for 30 s) and visible light (500 nm for 60 s) irradiations.

4. Dissipative particle dynamics (DPD) Simulations

The DPD method employed in the present work is a particle-based, mesoscale simulation technique. It was firstly introduced by Hoogerbrugge and Koelman in 1992[4] and improved by Español and Warren[5]. In the method, one DPD bead represents a group of atoms, and the motion of all beads in the system obeys Newton's equations of motion.

In DPD method, the force on bead *i* is consisted of conservative force $F_{ij}^{(C)}$, dissipative force $F_{ij}^{(D)}$, and random force $F_{ij}^{(R)}$.

$$F_{ij}(r_{ij}) = F_{ij}^{(C)}(r_{ij}) + F_{ij}^{(D)}(r_{ij}) + F_{ij}^{(R)}(r_{ij}) \quad (1)$$

The conservative force, dissipative force and random force are given by:

$$F_{ij}^{(C)} = -\alpha_{ij}\,\omega^{C}\left(r_{ij}\right)\vec{e}_{ij}, \tag{2}$$

$$F_{ij}^{(D)} = -\gamma\omega^{D}\left(r_{ij}\right)\left(\vec{v}_{ij}\cdot\vec{e}_{ij}\right)\vec{e}_{ij}, \tag{3}$$

$$F_{ij}^{(R)} = \sigma\omega^{R}\left(r_{ij}\right)\xi_{ij}\Delta t^{-1/2}\vec{e}_{ij}, \tag{4}$$

where $\vec{r}_{ij} = \vec{r}_i - \vec{r}_j$, $r_{ij} = \left|\vec{r}_{ij}\right|$, $\vec{e}_{ij} = \vec{r}_{ij} / r_{ij}$, $\vec{r}_i$ and $\vec{r}_j$ are the positions of bead i and bead j, respectively. $\vec{v}_{ij} = \vec{v}_i - \vec{v}_j$, $\vec{v}_i$ and $\vec{v}_j$ are the velocities of bead i and bead j, respectively. α_{ij} is a constant that describes the maximum repulsion between two interacting beads. γ and σ are the amplitudes of dissipative and random forces, respectively. ω^C, ω^D and ω^R are three weight functions for the conservative, dissipative, and random forces, respectively. For the conservative force, we choose $\omega_{ij}^C(r_{ij})=1-r_{ij}/R_c$ for $r_{ij}<R_c$ and $\omega_{ij}^C(r_{ij})=0$ for $r_{ij}\geq R_c$. According to the fluctuation-dissipation theorem, $\omega_{ij}^D(r_{ij})$ and $\omega_{ij}^R(r_{ij})$ follow a certain relation $\omega_{ij}^D(r)=[\omega_{ij}^R(r)]^2$ and $\sigma^2=2\gamma k_BT$ (σ=3 and γ=4.5), so that the system has a canonical equilibrium distribution. The following simple form of ω^D and ω^R was chosen according to Groot and Warren[6]:

$$\omega^{D}(r) = \begin{cases} (1-r/R_c)^2 & (r < R_c) \\ 0 & (r \geq R_c) \end{cases}. \tag{5}$$

ξ_{ij} in equation 4 is a random number with zero mean and unit variance, chosen independently for each interacting pair of beads at each time step Δt. A standard MD-like velocity-verlet algorithm is used here to integrate the equations of motion. For simplicity, the cutoff radius R_c, the bead mass m, and the temperature k_BT are taken as the units of the simulations, i.e., $R_c=m=k_BT=1$; thus the time unit $\tau=(mR_c^2/k_BT)^{1/2}=1$.

In our simulations, the azobenzene-functionalized graphene nanoribbons are modeled as a coarse-grained brush-like bead-spring chain, $A_xB_yC_z$, with x A-beads in the GNR backbone, y B-beads standing for other AZO aromatic rings and z C-beads standing for the terminal alkyl chains. As shown in Fig. 5 and Fig. S10, two coarse-grained models are constructed to investigate the self-assembly behaviors of GNR-AZO1 and GNR-AZO2 in THF solution. For these models, a harmonic spring force $\vec{F}_{ij}^{B} = -C^{B}(r_{ij} - r_{eq}^{B})\vec{e}_{ij}$ (C^B=100, $r_{eq}^{B} = 0.7$) is adopted between bonded beads i and j in the molecule. Meanwhile, the rigid-body constraint algorithm was employed to control the stiffness of the rod GNR backbone.

In the DPD simulation, the interaction parameter between the same type beads is set as $\alpha_{CC}=\alpha_{SS}=25$ to correctly describe the compressibility of THF. Considering that the π-π interactions between the GNR backbones are the main driving force for the GNR-AZOs self-assembly in THF.

The interaction parameters $\alpha_{AA}=\alpha_{BB}=5$ and $\alpha_{AB}=10$ are adopted. Meanwhile, $\alpha_{BC}=\alpha_{AS}=\alpha_{AC}=40$, $\alpha_{BS}=30$ and $\alpha_{CS}=26$ are employed to reflect the incompatibility between the GNR-AZOs and the solvent in our simulations. All the interaction parameters are listed in Table S2.

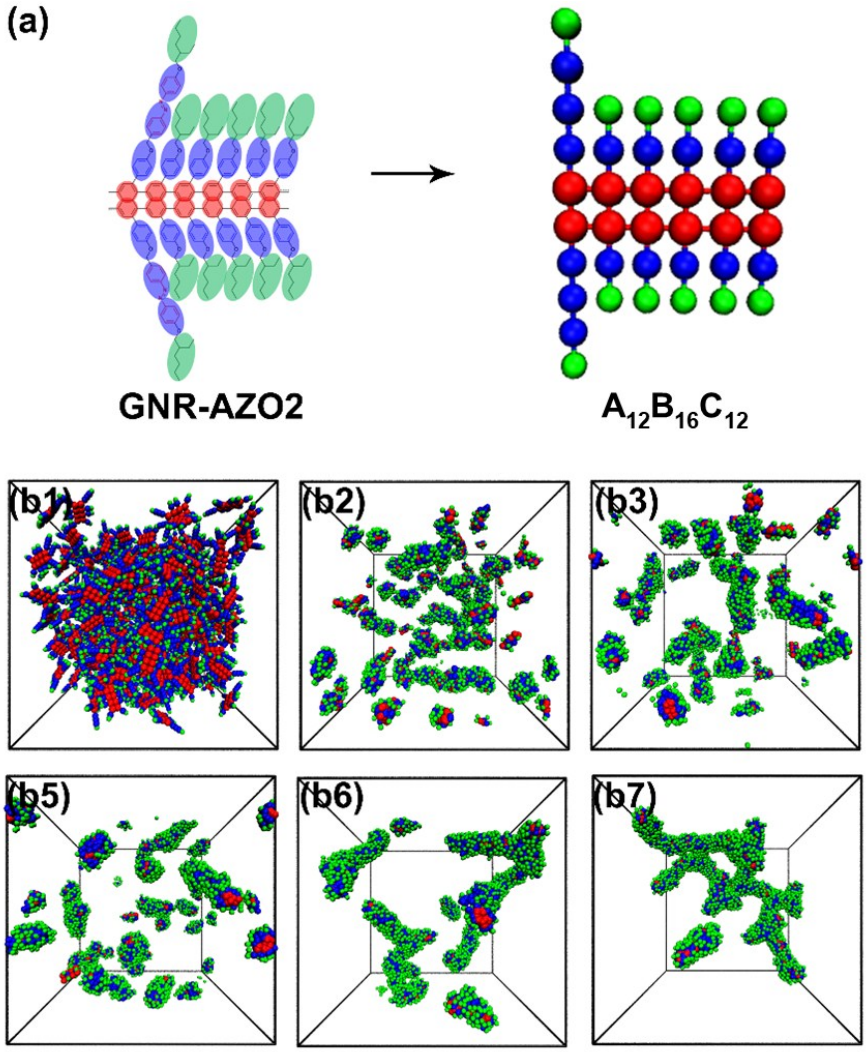

Fig. S10 DPD simulations of GNR-AZO2. (a) the coarse-grain mapping of GNR-AZO2; (b1−b6) The formation process of $A_{12}B_{16}C_{12}$ nanowires at different simulation times: (b1) t = 0; (b2) t= 2.0×10^4; (b3) t = 3.0×10^4; (b4) t = 5.0×10^4; (b5) t = 5.0×10^5; (b6) t = 2.0×10^6. Red, GNR backbone; blue, AZOs; green, alkyl chains.

Table S2. Conservative force constants αij used by DPD simulations.

	A (GNR)	B (AZO)	C (Alkyl chain)	S (THF)
A (GNR)	5.00			
B (AZO)	10.00	5.00		
C (Alkyl chain)	40.00	40.00	25.00	
S (THF)	40.00	30.00	26.00	25.00

All DPD simulations are performed in a cubic box of size 40×40×40 R_c^3 containing 1.92×10^5 beads by using Galamost package[7] on NVIDIA Tesla K20 GPU. The integration time step of 0.04 is utilized and the total simulation steps are 5×10^6 for each simulation. Also, a series of simulations with different random seeds were performed. It shows that the results are reproducible. All figures of the molecular structures were drawn using the VMD[8] program (v.1.9.3).

5. ^{1}H NMR and^{13}C NMR Spectra

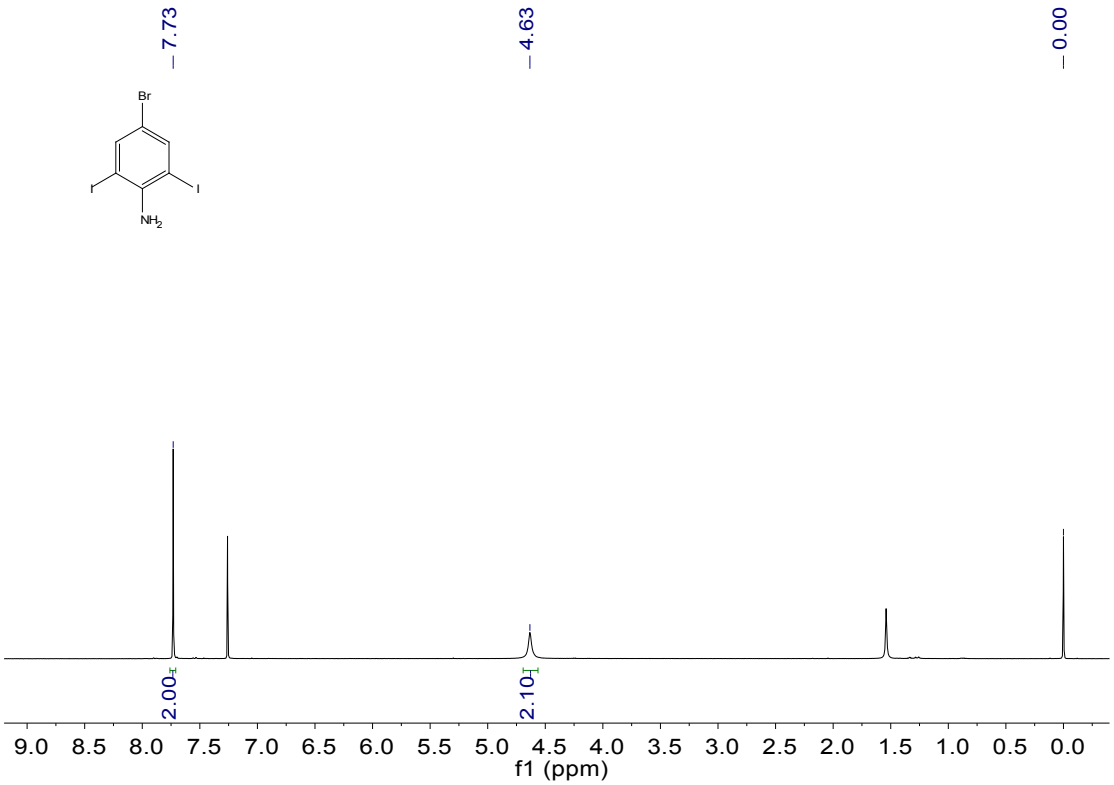

Fig. S11 ^{1}H NMR spectra of compound 2 in $CDCl_3$.

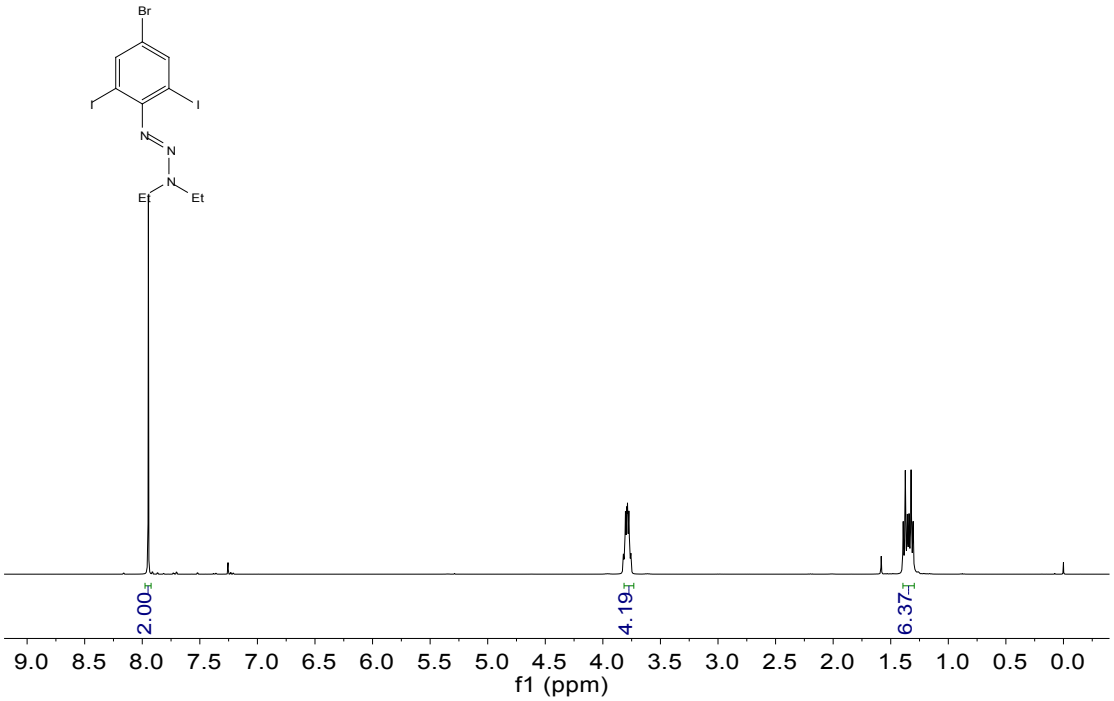

Fig. S12 ^{1}H NMR spectra of compound 3 in $CDCl_3$.

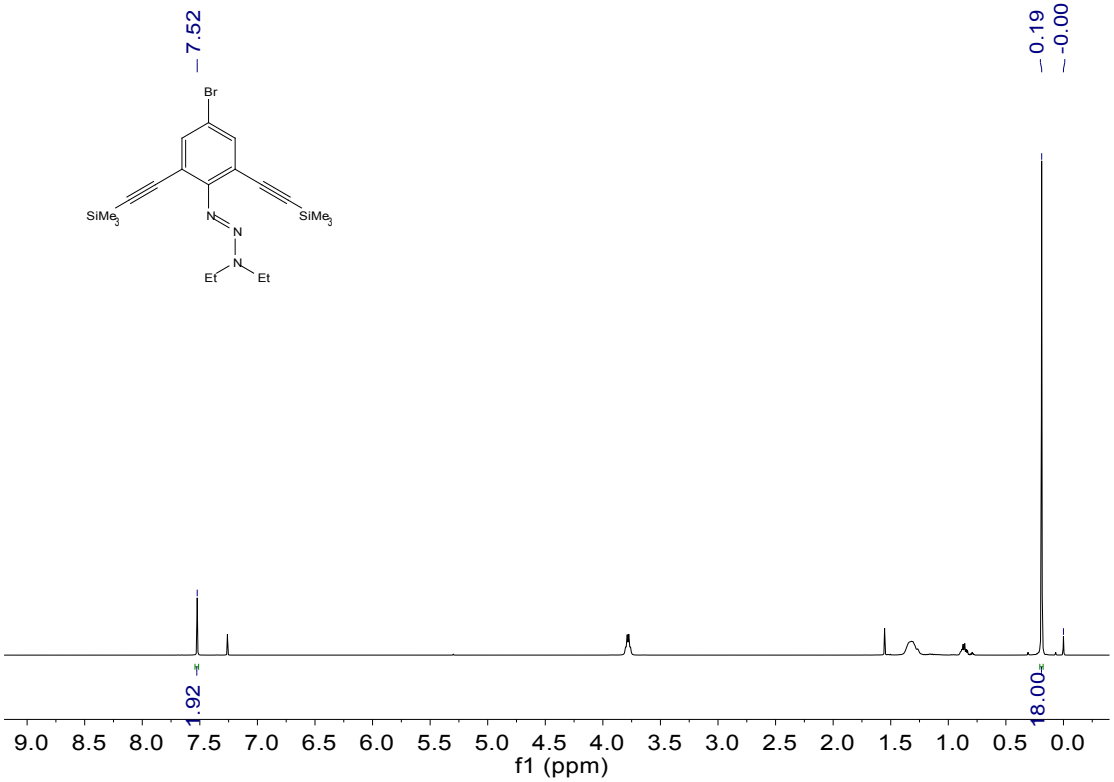

Fig. S13 ^{1}H NMR spectra of compound 4 in $CDCl_3$.

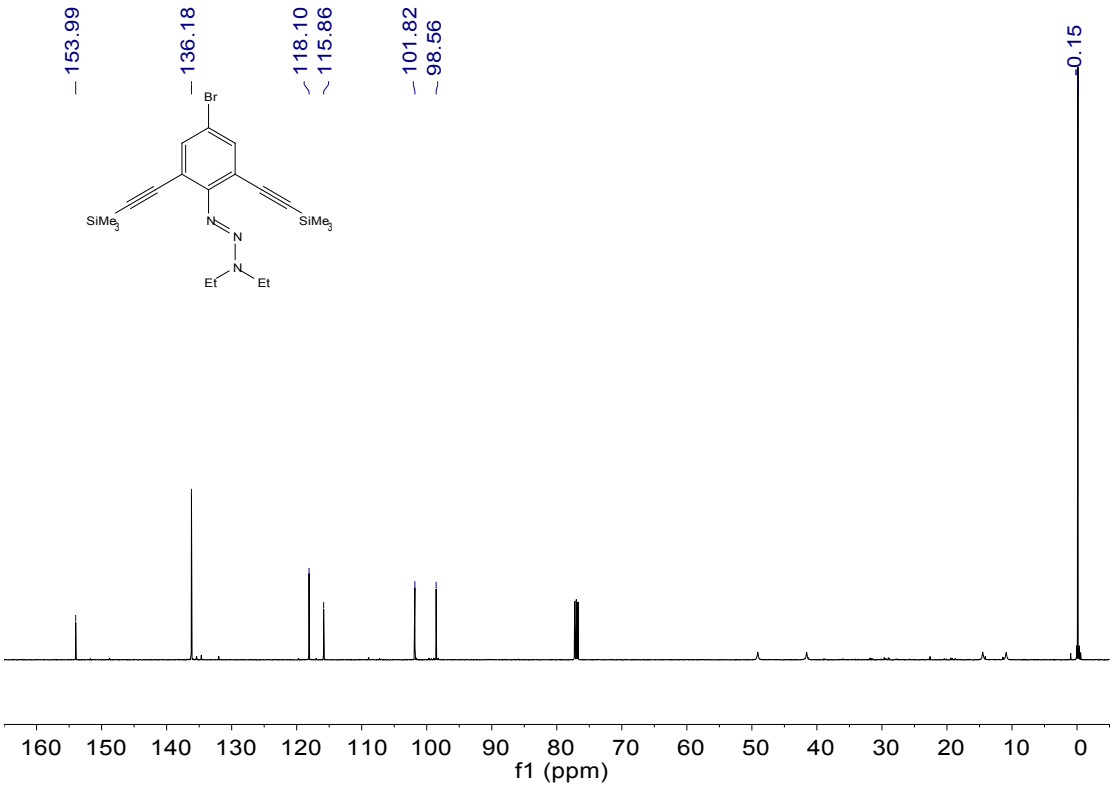

Fig. S14 ^{13}C NMR spectra of compound 4 in $CDCl_3$.

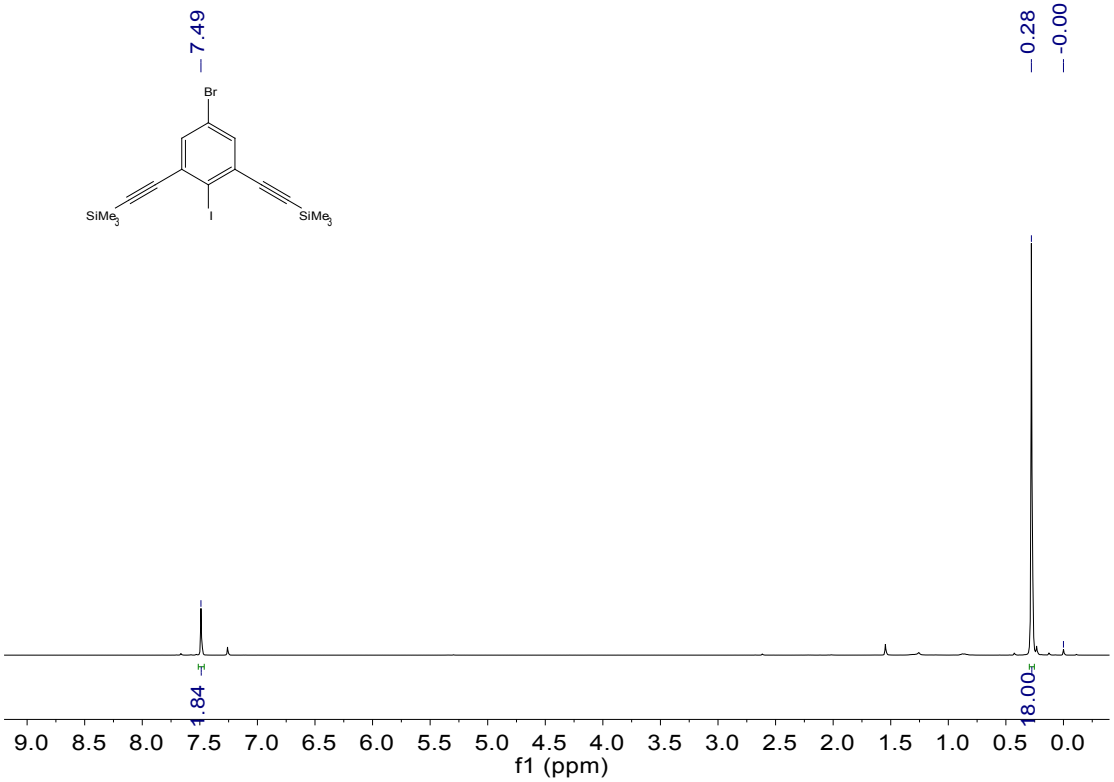

Fig. S15 ^{1}H NMR spectra of compound 5 in $CDCl_3$.

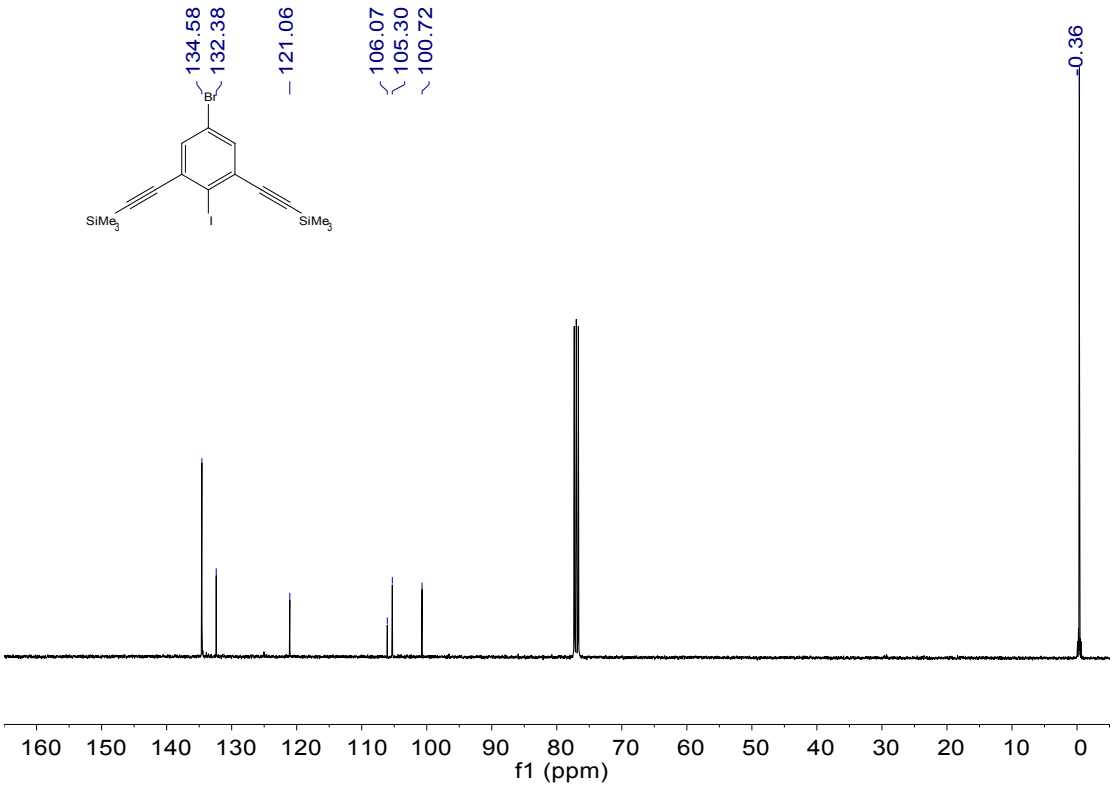

Fig. S16 ^{13}C NMR spectra of compound 5 in $CDCl_3$.

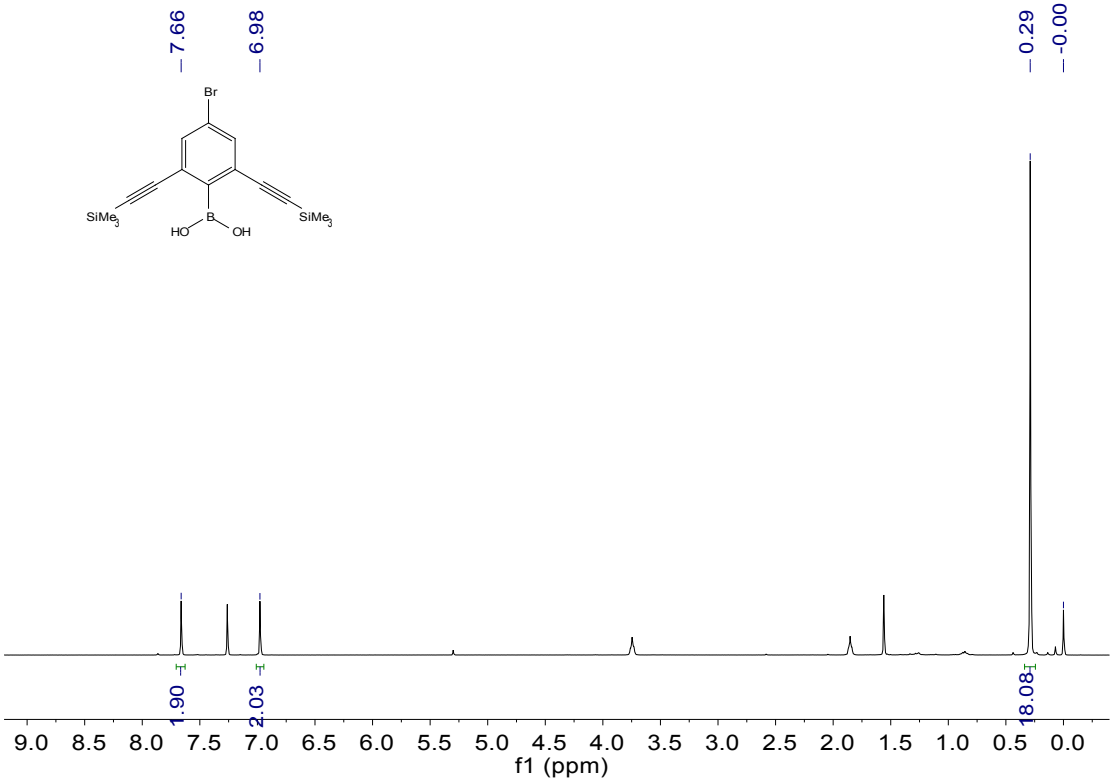

Fig. S17 ^{1}H NMR spectra of compound 6 in $CDCl_3$.

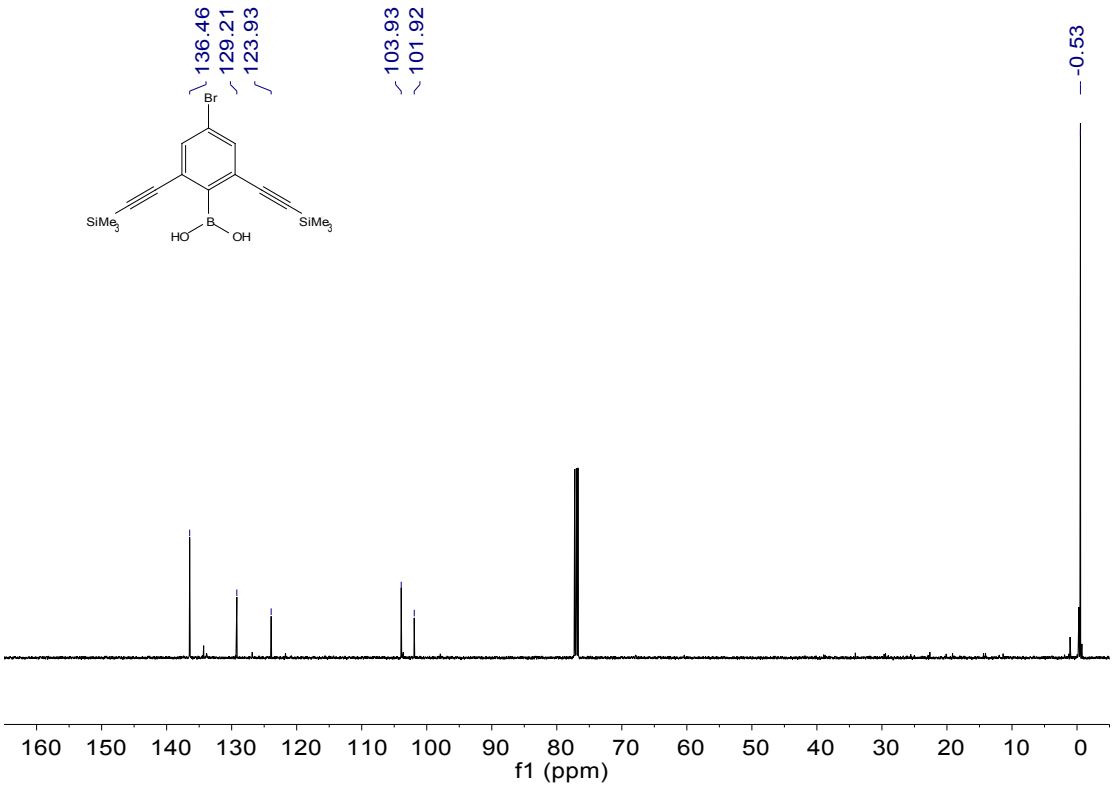

Fig. S18 ^{13}C NMR spectra of compound 6 in $CDCl_3$.

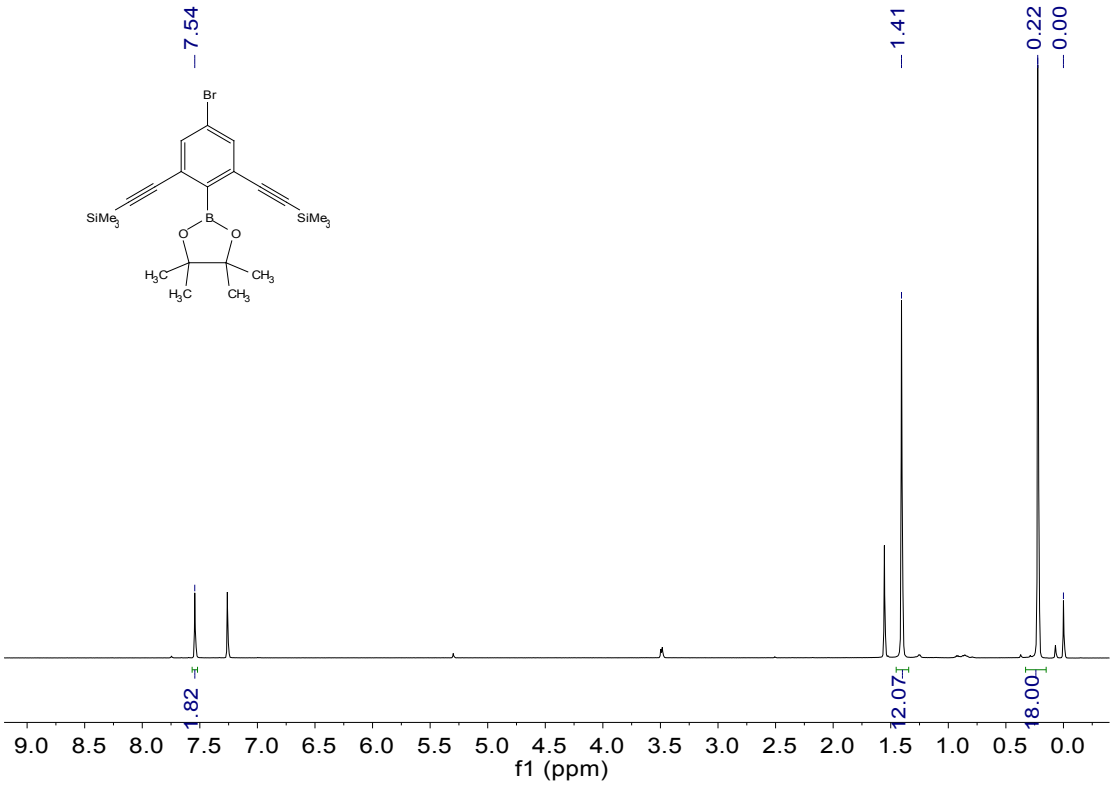

Fig. S19 ^{1}H NMR spectra of compound 7 in $CDCl_3$.

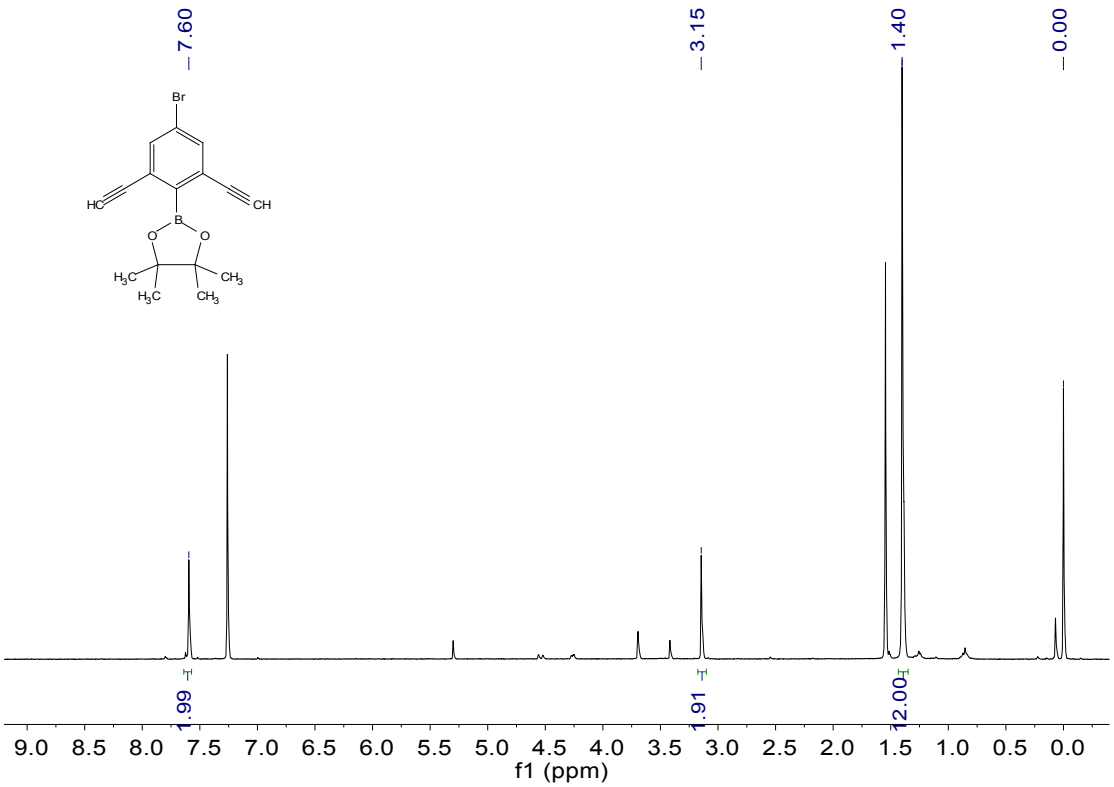

Fig. S20 ^{1}H NMR spectra of compound 8 in $CDCl_3$.

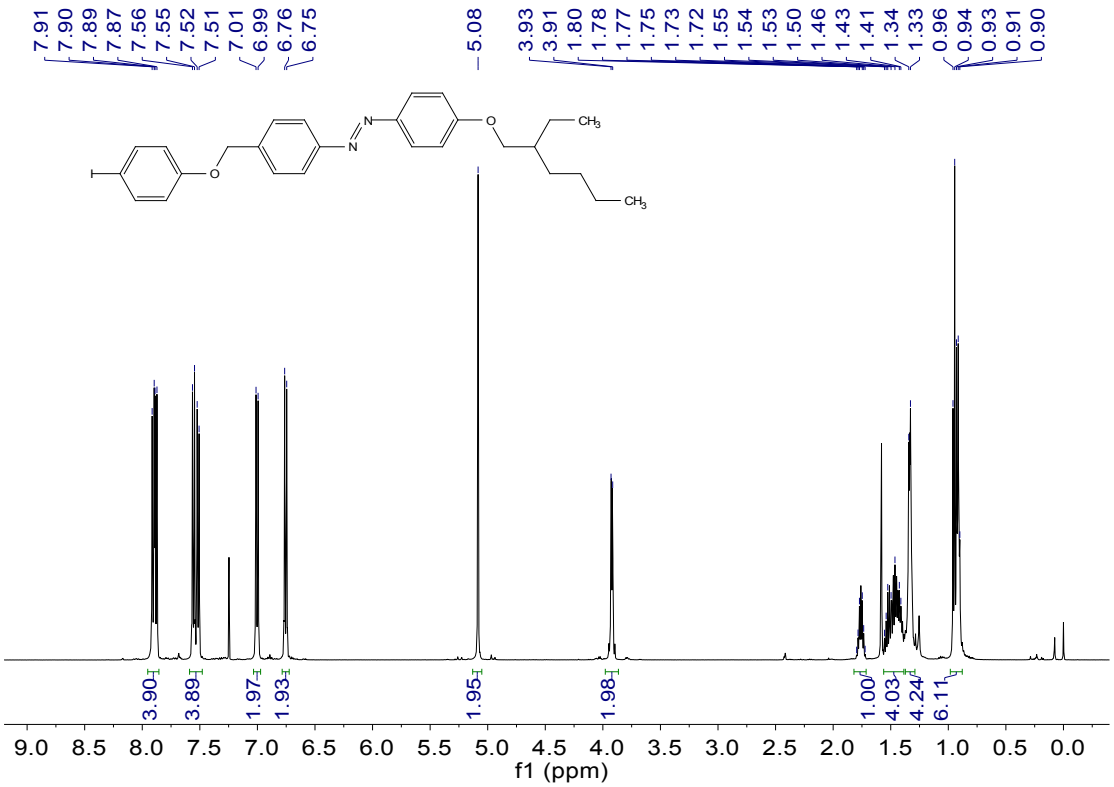

Fig. S21 ^{1}H NMR spectra of compound A4 in $CDCl_3$.

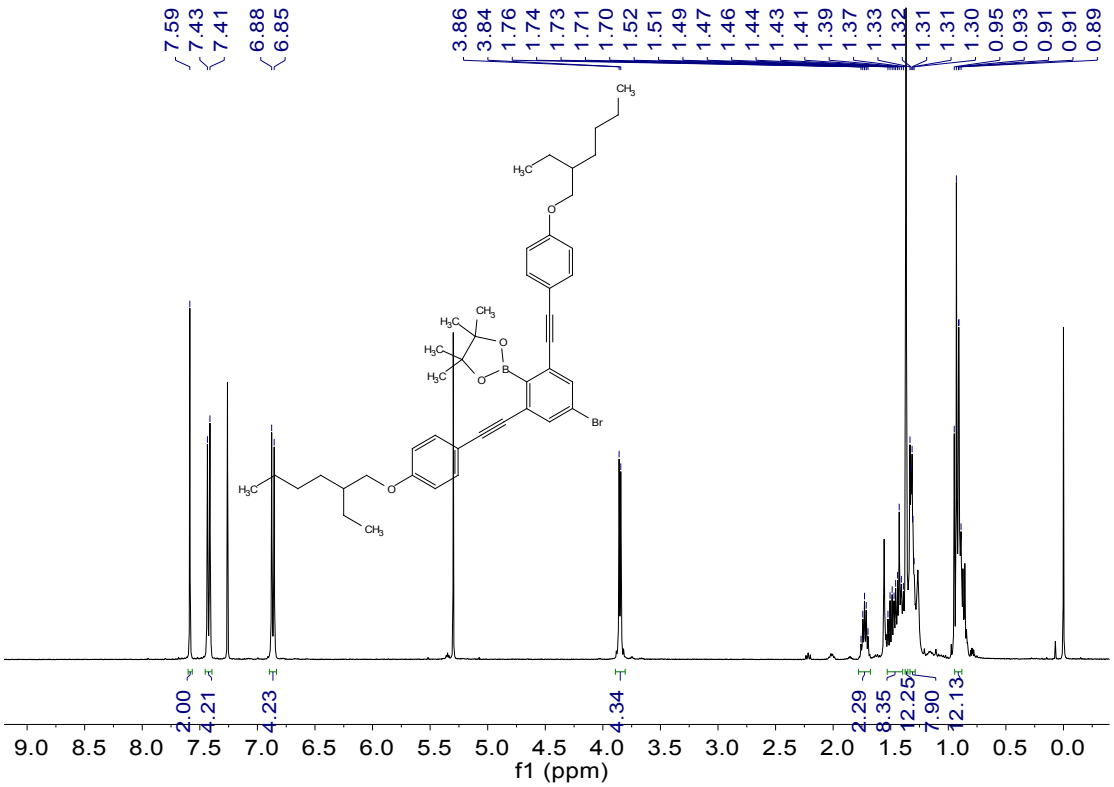

Fig. S22 ^{1}H NMR spectra of monomer 10 in $CDCl_3$.

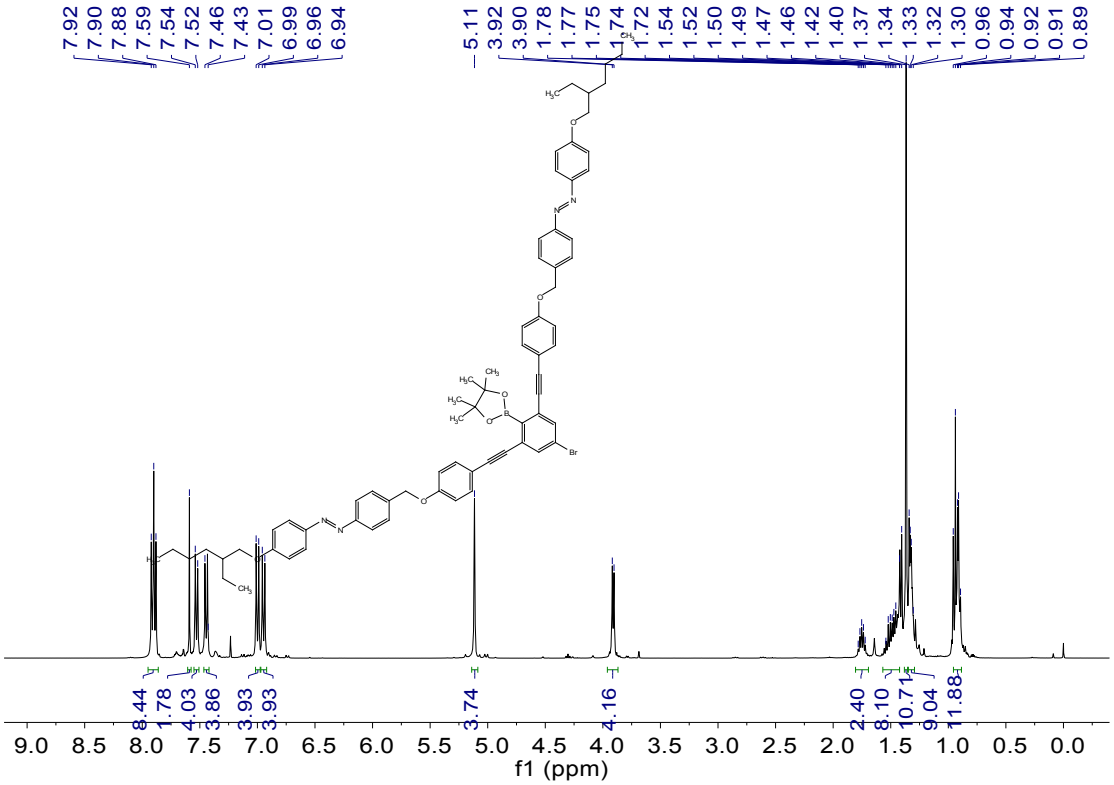

Fig. S23 ^{1}H NMR spectra of monomer 9 in $CDCl_3$.

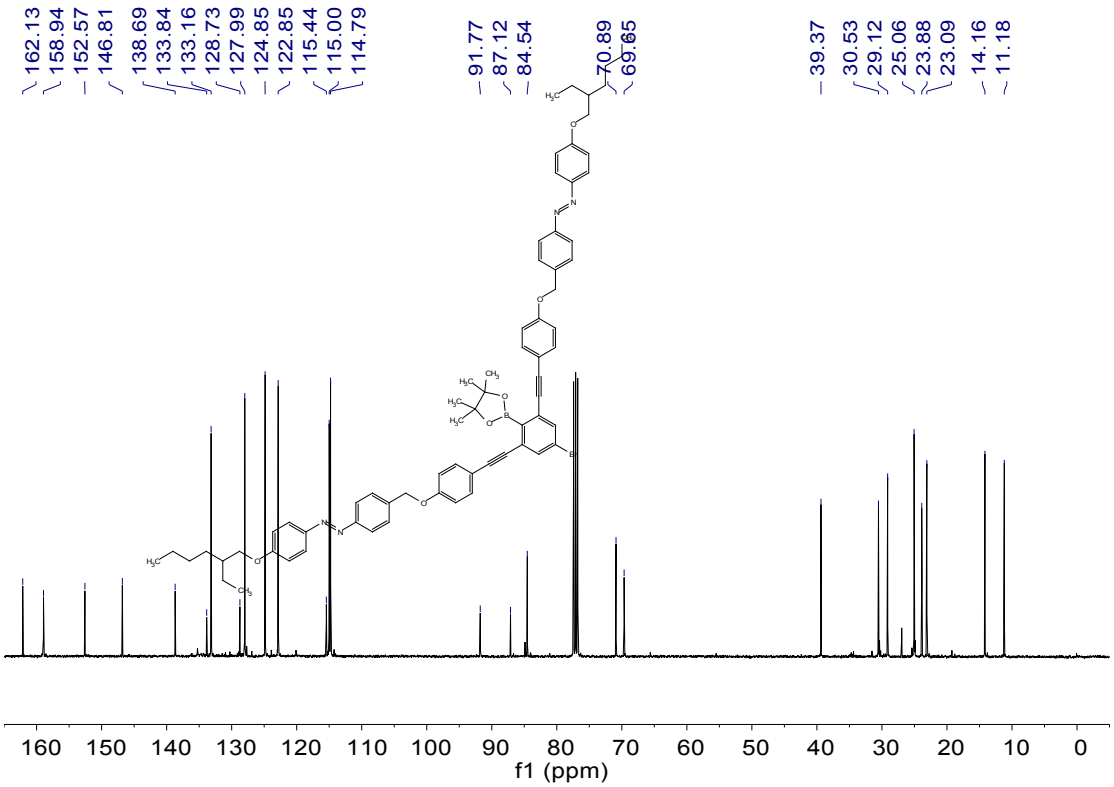

Fig. S24 ^{13}C NMR spectra of monomer 9 in $CDCl_3$.

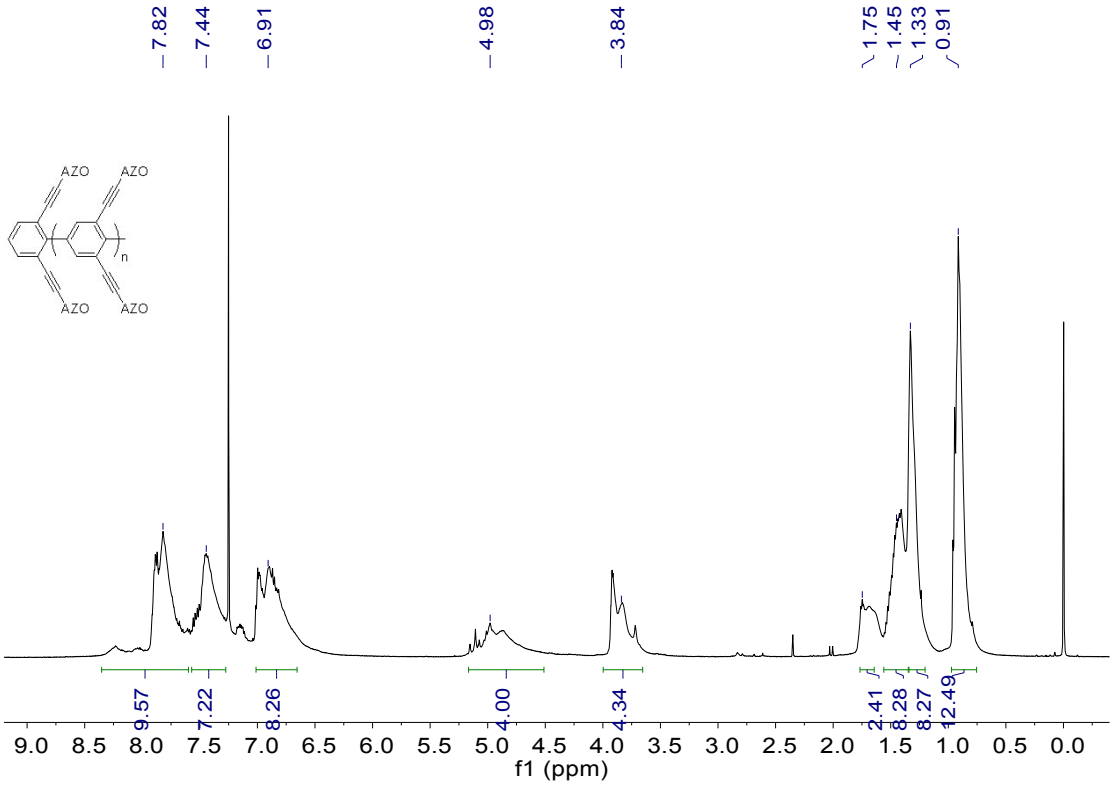

Fig. S25 ^{1}H NMR spectra of PDAPP-AZO1 in $CDCl_3$.

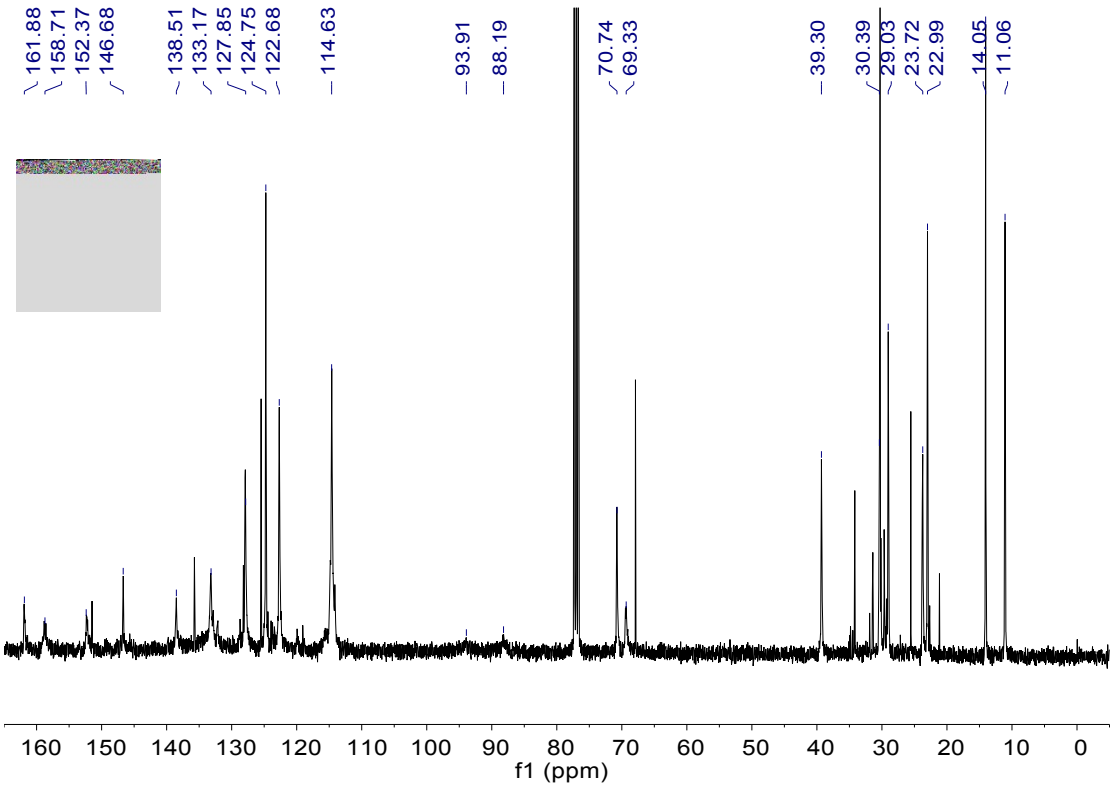

Fig. S26 ^{13}C NMR spectra of PDAPP-AZO1 in $CDCl_3$.

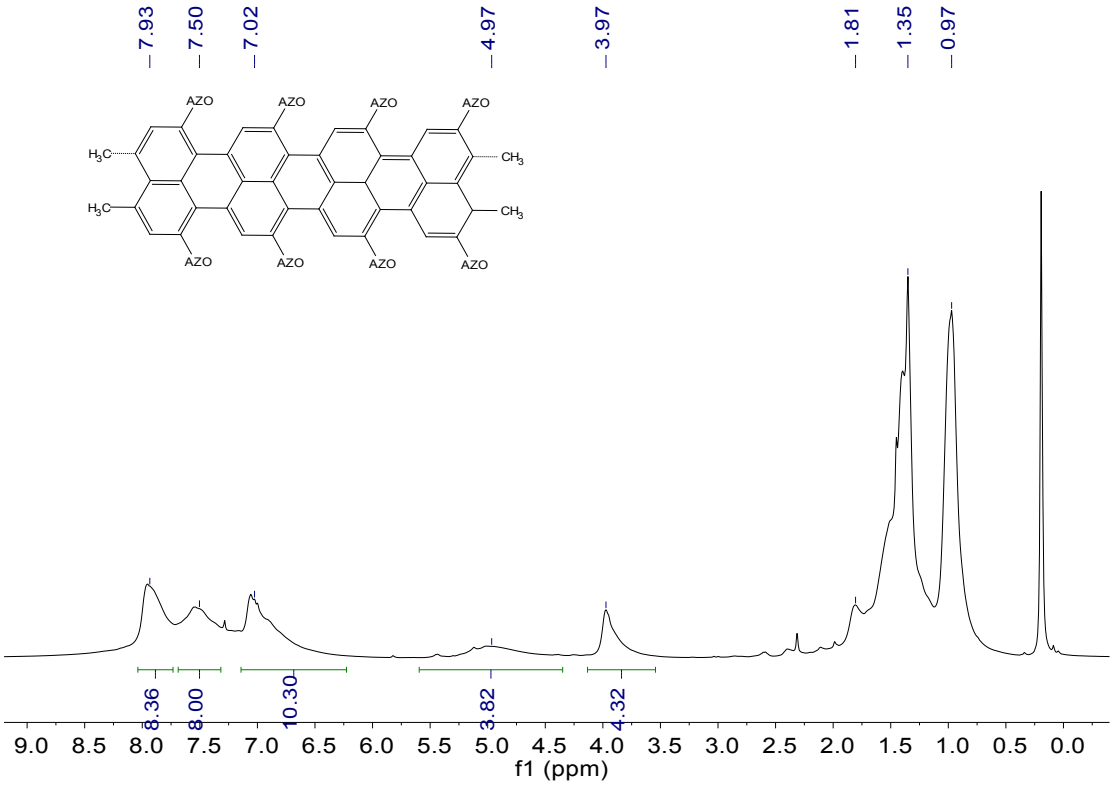

Fig. S27 ^{1}H NMR spectra of GNR-AZO1 in $CDCl_3$.

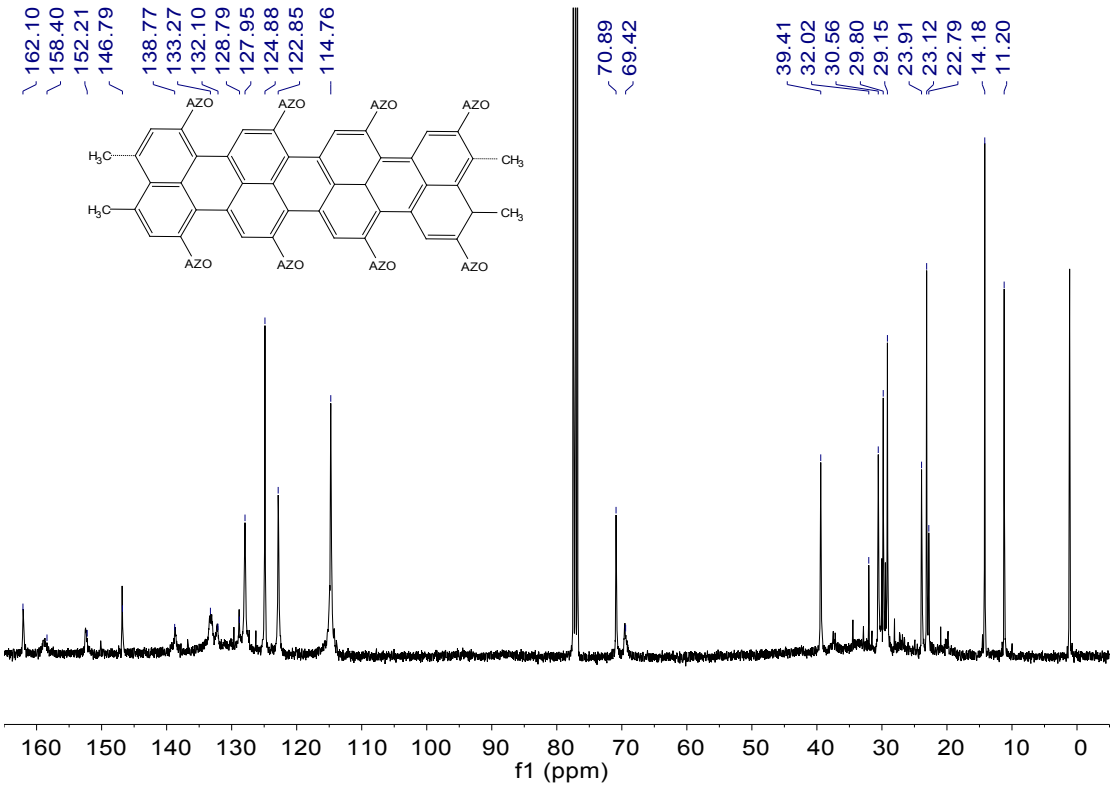

Fig. S28 ^{13}C NMR spectra of GNR-AZO1 in $CDCl_3$.

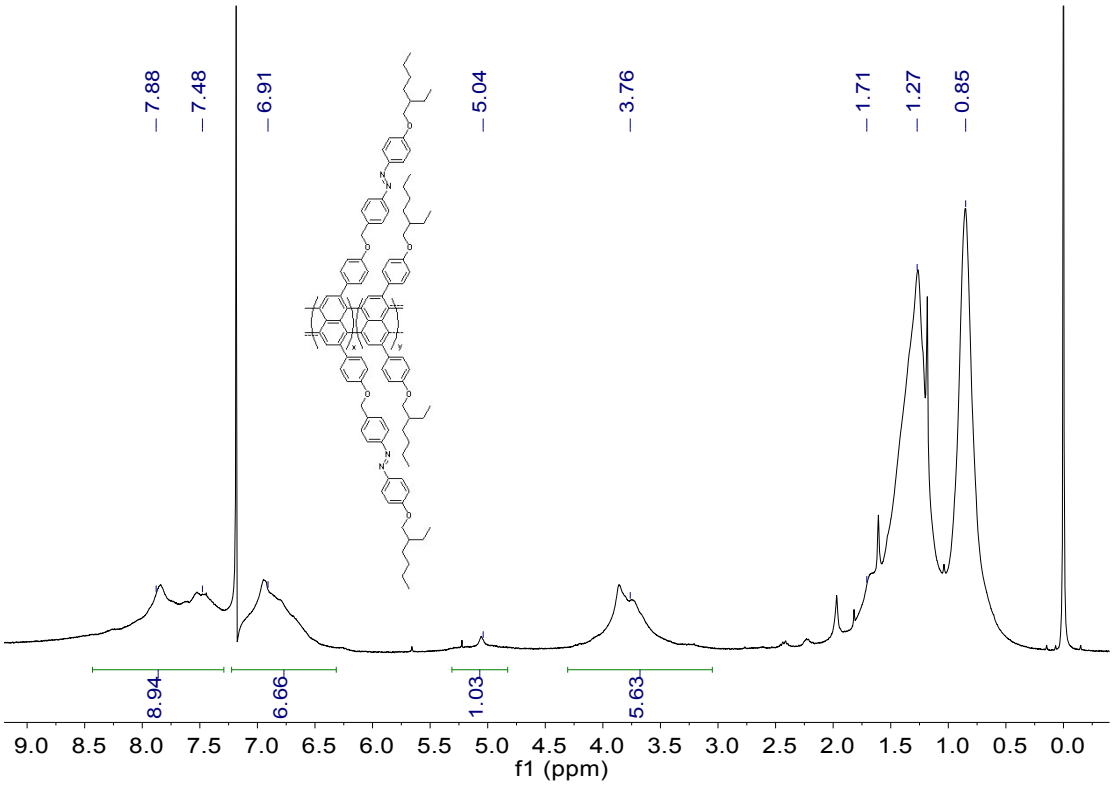

Fig. S29 ^{1}H NMR spectra of GNR-AZO2 in $CDCl_3$.

References

1. F. Li, Y.-Z. Zhu, S.-C. Zhang, H.-H. Gao, B. Pan and J.-Y. Zheng, *Dyes and Pigments*, 2017, **139**, 292-299.
2. W. Yang, A. Lucotti, M. Tommasini and W. A. Chalifoux, *Journal of the American Chemical Society*, 2016, **138**, 9137-9144.
3. J. Tian, L. Fu, Z. Liu, H. Geng, Y. Sun, G. Lin, X. Zhang, G. Zhang and D. Zhang, *Advanced Functional Materials*, 2019, **29**, 1807176.
4. P. J. Hoogerbrugge and J. M. V. A. Koelman, *Europhysics Letters (EPL)*, 1992, **19**, 155-160.
5. P. Español and P. Warren, *Europhysics Letters (EPL)*, 1995, **30**, 191-196.
6. R. D. Groot and P. B. Warren, *The Journal of Chemical Physics*, 1997, **107**, 4423-4435.
7. Y.-L. Zhu, H. Liu, Z.-W. Li, H.-J. Qian, G. Milano and Z.-Y. Lu, *Journal of Computational Chemistry*, 2013, **34**, 2197-2211.
8. W. Humphrey, A. Dalke and K. Schulten, *Journal of molecular graphics*, 1996, **14**, 33-38.